molbank

MDPI

Short Note

2-([1,1′-Biphenyl]-4-yl)-5-[(*E*)-2-(3-methoxy-1-phenyl-1*H*-pyrazol-4-yl)ethenyl]-3,3-dimethyl-3*H*-indole

Gabrielė Varvuolytė [1,2], Aurimas Bieliauskas [2], Neringa Kleizienė [2], Asta Žukauskaitė [1,3,*] and Algirdas Šačkus [1,2,*]

[1] Department of Organic Chemistry, Kaunas University of Technology, LT-50254 Kaunas, Lithuania; gabriele.varvuolyte@ktu.edu
[2] Institute of Synthetic Chemistry, Kaunas University of Technology, LT-51423 Kaunas, Lithuania; aurimas.bieliauskas@ktu.lt (A.B.); neringa.kleiziene@ktu.lt (N.K.)
[3] Department of Chemical Biology, Faculty of Science, Palacký University, CZ-77900 Olomouc, Czech Republic
* Correspondence: asta.zukauskaite@upol.cz (A.Ž.); algirdas.sackus@ktu.lt (A.Š.)

Abstract: The ligandless palladium-catalyzed Heck reaction of 4-ethenyl-3-methoxy-1-phenyl-1*H*-pyrazole and 2-([1,1′-biphenyl]-4-yl)-5-bromo-3,3-dimethyl-3*H*-indole gave the previously unreported 2-([1,1′-biphenyl]-4-yl)-5-[(*E*)-2-(3-methoxy-1-phenyl-1*H*-pyrazol-4-yl)ethenyl]-3,3-dimethyl-3*H*-indole in 45% yield. The compound was characterized using NMR, FT-IR spectroscopy, and HRMS data. The optical properties of the compound were investigated in tetrahydrofuran by UV-Vis and fluorescence spectroscopy.

Keywords: biphenyl; indole; pyrazole; Heck reaction; fluorescence

Citation: Varvuolytė, G.; Bieliauskas, A.; Kleizienė, N.; Žukauskaitė, A.; Šačkus, A. 2-([1,1′-Biphenyl]-4-yl)-5-[(*E*)-2-(3-methoxy-1-phenyl-1*H*-pyrazol-4-yl)ethenyl]-3,3-dimethyl-3*H*-indole. *Molbank* **2024**, *2024*, M1927. https://doi.org/10.3390/M1927

Academic Editor: Marcus Baumann

Received: 15 November 2024
Revised: 24 November 2024
Accepted: 25 November 2024
Published: 28 November 2024

1. Introduction

Biphenyl fragment-possessing compounds have shown a wide range of possible applications. For example, certain biphenyl derivatives were reported to be potential materials for organic light-emitting diodes [1,2] and solar cells [3,4]. Axially chiral biphenyl ligands are widely used in asymmetric synthesis or homogeneous catalysis [5,6]. Notably, biphenyl is considered to be a privileged scaffold in medicinal chemistry for ligand binding in hydrophobic pockets and the formation of π-π interactions with amino acids [7]. Natural biphenyl products, as well as synthetic derivatives display a broad range of biological activities. A number of biphenyl compounds, including flurbiprofen (Figure 1, example **I**), have been approved for clinical use [8]. Biphenyl-pyridine hybrid **II** inhibits the PD-1/PD-L1 interaction and shows anti-tumor activity in vivo [9]. Moreover, a pyrazole-biphenyl derivative **III** has been demonstrated to have an inhibitory activity against histone deacetylases and in vitro anti-cancer activity against several tested cell lines [10]. An indole-biphenyl carboxylic acid conjugate **IV** was found to target the peroxisome proliferator-activated receptor PPARγ, indicating an anti-diabetic activity [11]. Biphenyl derivative **V**, containing a distinctive 1,3a,6a-triazapentalene moiety, has emerged as a fluorescent probe for the visualization and simultaneous inhibition of kinesin spindle protein inside cells [12]. Pyrazoles with 3- and 5-biphenyl substituents show blue fluorescence emission in solution and high fluorescence quantum yields Φ_f, especially the compound **VI**, for which Φ_f reaches a remarkable value of 0.97 [13]. Moreover, 2-([1,1′-biphenyl]-4-yl)-3,3-dimethyl-3*H*-indole **VII** was employed in the preparation of a biphenyl-substituted indolo[2,1-*b*][1,3]benzoxazine as a potential bichromophoric photochrome [14].

In the past, we have introduced new fluorescent biphenyl-coupled pyrazole and aryl coupled indole derivatives [15,16]. Thus, as a continuation of our previous work, we synthesized a fluorescent pyrazole-indole hybrid with a biphenyl fragment, 2-([1,1′-biphenyl]-4-yl)-5-[(*E*)-2-(3-methoxy-1-phenyl-1*H*-pyrazol-4-yl)ethenyl]-3,3-dimethyl-3*H*-indole (**3**)

through the palladium-catalyzed Heck cross coupling reaction. The structure of the new compound was elucidated through NMR, FT-IR spectroscopy, and HRMS.

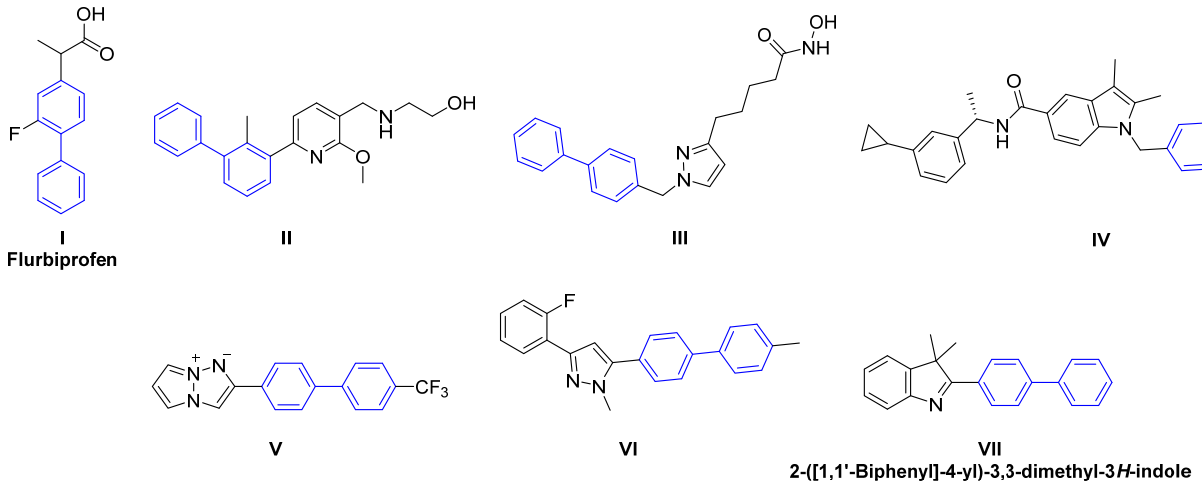

Figure 1. Examples of biphenyl-containing compounds.

2. Results and Discussion

Typically, biphenyl or its derivatives are synthesized using Ullmann, Kumada, Suzuki-Miyaura, Stille, Negishi cross couplings, which involve transition metals, such as palladium [8,17]. A one-pot Heck/Suzuki coupling, using palladium(II) acetate, tetrabutylammonium salts, and cesium carbonate, was successfully applied in the synthesis of (*E*)-4-styryl-biphenyl [18].

The starting materials 4-ethenyl-3-methoxy-1-phenyl-1*H*-pyrazole (**1**) [19] and 2-([1,1′-biphenyl]-4-yl)-5-bromo-3,3-dimethyl-3*H*-indole (**2**), which was synthesized from 4-bromophenylhydrazine hydrochloride and 1-([1,1′-biphenyl]-4-yl)-2-methylpropan-1-one through the Fischer indole synthesis reaction, were subjected to a ligandless palladium-catalyzed Heck reaction. Tetrabutylammonium chloride (TBAC) acted as the phase-transfer catalyst, and cesium carbonate was employed as the base. After column chromatography, target compound **3** was obtained in 45% yield (Scheme 1).

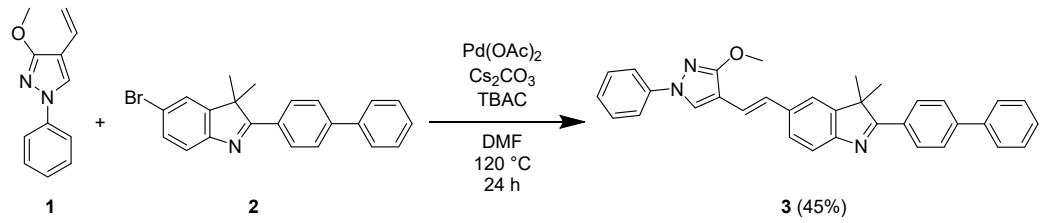

Scheme 1. Synthesis of compound **3.**

Comprehensive structural determination data for compounds 2 and 3 are provided in the Supplementary Materials (Figures S1–S15). The structure of compound **3** was elucidated through the use of a combination of standard and advanced NMR techniques, namely, ^{1}H-^{1}H COSY, ^{1}H-^{1}H TOCSY, ^{1}H-^{1}H NOESY, ^{1}H-^{13}C HSQC, ^{1}H-^{13}C H2BC, ^{1}H-^{13}C HMBC, ^{1}H-^{15}N LR-HSQMBC, and 1,1-ADEQUATE. The relevant chemical shifts and correlations are depicted in Figure 2. For instance, the well-resolved geminal 3-$(CH_3)_2$ group protons (δ 1.66 ppm, singlet) from the indole moiety showed NOEs with the neighboring biphenyl 3,5-H (δ 8.25 ppm, doublet) and indole 4-H (δ 7.45–7.49 ppm) protons. Moreover, other distinct NOEs were exhibited between the pyrazole ring proton 5-H (δ 7.86 ppm, singlet) and the neighboring phenyl group (δ 7.61–7.64 ppm) and ethene bridge H_a (δ 6.97 ppm) protons, which confirms their proximity in space. This information allowed all the distinct

^{1}H spin systems to be easily resolved by carefully analyzing the ^{1}H-^{1}H COSY and ^{1}H-^{1}H TOCSY spectral data.

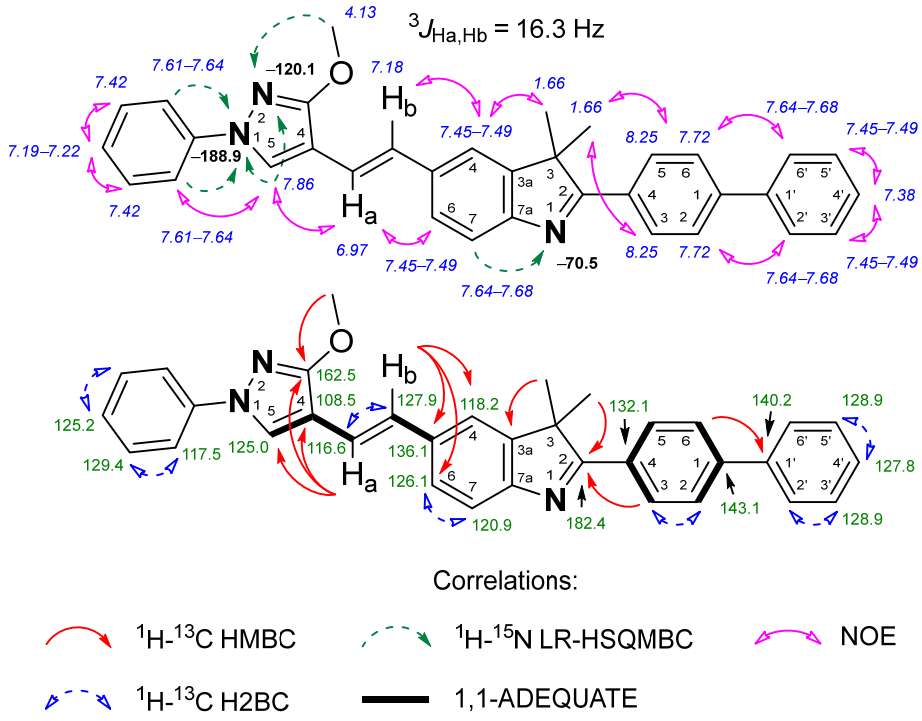

Figure 2. Relevant ^{1}H-^{13}C HMBC, ^{1}H-^{13}C H2BC, ^{1}H-^{15}N LR-HSQMBC, ^{1}H-^{1}H NOESY, and 1,1-ADEQUATE correlations, as well as ^{1}H NMR (in italics), ^{13}C NMR, and ^{15}N NMR (bold) chemical shifts in compound **3**.

The ^{15}N NMR spectral data were obtained through the ^{1}H-^{15}N LR-HSQMBC (long-range heteronuclear single-quantum multiple-bond correlation) experiment, which further supported the assignment of the aforementioned ^{1}H spin systems. For instance, the indole ring proton 7-H (δ 7.64–7.68 ppm) showed a long-range correlation with the indole nitrogen (δ −70.5 ppm), while the pyrazole ring proton 5-H (δ 7.86 ppm) had long-range correlations with both N-1 "pyrrole-like" (δ −188.9 ppm) and N-2 "pyridine-like" (δ −120.1 ppm) nitrogen atoms.

Lastly, unambiguous assignments of the ^{13}C NMR resonances were obtained via long-range correlations in the ^{1}H-^{13}C HMBC and ^{1}H-^{13}C H2BC spectra, which, in combination with the data from the ^{1}H-^{13}C HSQC and 1,1-ADEQUATE experiments, allowed different structural fragments to be joined. Namely, the ethene bridge protons H_a (δ 6.97 ppm, doublet, $^{3}J_{Ha,Hb}$ = 16.3 Hz), and H_b (δ 7.18 ppm, doublet, $^{3}J_{Ha,Hb}$ = 16.3 Hz) exhibited long-range ^{1}H-^{13}C HMBC correlations with their neighboring heterocyclic moieties. Then, with the addition of 1,1-ADEQUATE spectral data, it was evident that the protonated CH_a carbon (δ 116.6 ppm) was adjacent to the pyrazole carbon C-4 (δ 108.5 ppm). At the same time, the CH_b carbon (δ 127.9 ppm) correlated with the adjacent indole carbon C-5 (δ 136.1 ppm).

The optical properties of compound **3** were investigated in tetrahydrofuran (Figure 3). The UV-Vis absorption maximum λ_{max} is situated at 384 nm, and the emission maximum λ_{em} is in the blue-green part of the visible light spectrum, at 492 nm, giving a Stokes shift value of 108 nm. Compared to the previously reported structurally similar pyrazole-indole hybrids, which exhibit their UV-Vis absorption maxima in the range of 368–375 nm, and fluorescence maxima at 462–480 nm [19], compound **3** possesses obvious bathochromic shifts for both absorption and fluorescence maxima. The fluorescence quantum yield Φ_f for compound **3** was estimated to be 69.2%.

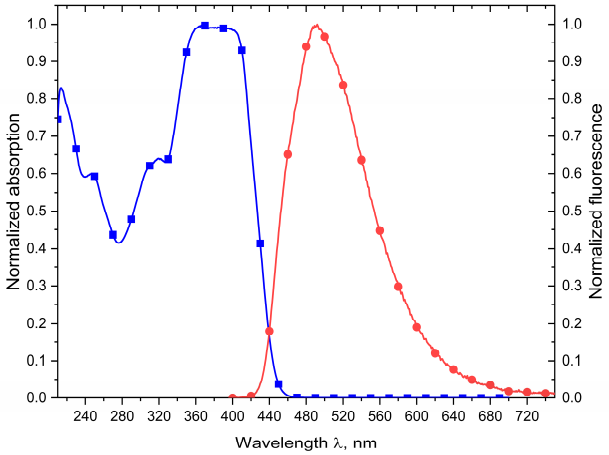

Figure 3. UV-Vis absorption (blue) and fluorescence emission (red) spectra of compound **3** in tetrahydrofuran (excitation wavelength λ_{ex}—380 nm).

3. Materials and Methods

All chemicals and solvents were purchased from commercial suppliers (Labochema, Vilnius, Lithuania and Eurochemicals, Vilnius, Lithuania) and used without further purification. NMR spectra were recorded in $CDCl_3$ solutions at 25 °C on a Bruker Avance III 700 (700 MHz for ^{1}H, 176 MHz for ^{13}C, 71 MHz for ^{15}N) spectrometer equipped with a 5 mm TCI ^{1}H-^{13}C/^{15}N/D z-gradient cryoprobe (Bruker Bio-Spin AG, Fällanden, Switzerland) and processed on TopSpin 3.6.4 and MestReNova 11.0 software. The chemical shifts, expressed in ppm, were relative to tetramethylsilane (TMS). The ^{15}N NMR (^{1}H-^{15}N LR-HSQMBC) spectrum was referenced to neat, external nitromethane (coaxial capillary). The FT-IR spectrum was collected using the ATR method on a Bruker Vertex 70v spectrometer (Bruker Optik GmbH, Ettlingen, Germany) with an integrated Platinum ATR accessory and processed on OPUS 7.2 software. The melting points were determined in an open capillary tube with a Buchi M-565 apparatus (Büchi Labortechnik AG, Flawil, Switzerland) and are uncorrected (temperature gradient—2 °C/min). The high-resolution mass spectrometry (HRMS) spectrum was obtained in ESI mode on a Bruker MicrOTOF-Q III spectrometer (Bruker Daltonik GmbH, Bremen, Germany) and processed with Bruker Compass DataAnalysis 4.1 software. The reaction progress was monitored by TLC analysis on Macherey-Nagel™ ALUGRAM® Xtra SIL G/UV254 plates. TLC plates were visualized with UV light (wavelengths 254 and 365 nm). Compounds were purified by flash chromatography in a glass column (stationary phase—silica gel 60, 0.063–0.200 mm, 70–230 mesh ASTM, Merck KGaA, Darmstadt, Germany).

The UV–Vis spectrum of the 10^{-4} M solution in THF was recorded on a Shimadzu 2600 UV/Vis spectrophotometer (Shimadzu Corporation, Kyoto, Japan). The fluorescence spectrum was recorded on an FLS920 fluorescence spectrometer from Edinburgh Instruments (Edinburgh Analytical Instruments Limited, Edinburgh, UK). The fluorescence quantum yield was estimated from dilute THF solutions by an absolute method using the Edinburgh Instruments integrating sphere excited with a Xe lamp. The optical densities of the sample solutions were maintained below 0.1 to avoid reabsorption effects. All optical measurements were performed at room temperature under ambient conditions.

Synthesis of 2-([1,1′-biphenyl]-4-yl)-5-bromo-3,3-dimethyl-3H-indole (**2**)*:*

A mixture of 4-bromophenylhydrazine hydrochloride (1000 mg, 4.5 mmol, 1 eq.) and 1-([1,1′-biphenyl]-4-yl)-2-methylpropan-1-one (1505 mg, 6.75 mmol, 1.5 eq) was dissolved in ethanol (10 mL) and refluxed for 3 h. Then, a solution of sulfuric acid in ethanol (1 mL in 10 mL of ethanol, 1/10 v/v) was added dropwise. The reaction was stirred at reflux temperature for 24 h. The mixture was cooled, poured into distilled water (150 mL), and extracted with dichloromethane (4 × 25 mL). The organic layer was dried with anhydrous sodium sulfate, filtered, and concentrated under reduced pressure. The residue was purified

by column chromatography on silica gel (eluent—EtOAc/Hex 1/12 *v*/*v*). Yellowish solid; yield 75% (1268 mg); m.p. 167–169 °C; R_f = 0.50 (EtOAc/Hex 1/12 *v*/*v*). ^{1}H NMR (700 MHz, $CDCl_3$): δ 8.22 (d, *J* = 7.9 Hz, 2H), 7.72 (d, *J* = 7.9 Hz, 2H), 7.66 (d, *J* = 7.3 Hz, 2H), 7.56 (d, *J* = 7.9 Hz, 1H), 7.51—7.45 (m, 4H), 7.39 (t, *J* = 7.4 Hz, 1H), 1.62 (s, 6H). ^{13}C NMR (176 MHz, $CDCl_3$): δ 183.0, 152.2, 149.8, 143.5, 140.1, 131.6, 130.9, 128.9, 128.8, 127.9, 127.3, 127.1, 124.5, 122.2, 119.5, 53.9, 24.7. IR (ATR): 3083, 3056, 3027, 2984, 2964, 2928, 2863 (CH_{arom}, CH_{aliph}), 1509, 1483, 1459, 1444, 1406, 1329, 1249, 1214, 846, 825, 769, 736, 695 (C=C, CH_3 bending, C-N, CH_{arom} oop bending). HRMS (*m*/*z*): $[M+H]^+$ calcd. for $C_{22}H_{19}BrN$, 376.0695; found, 376.0699.

Synthesis of 2-([1,1′-biphenyl]-4-yl)-5-[(E)-2-(3-methoxy-1-phenyl-1H-pyrazol-4-yl)ethenyl]-3,3-dimethyl-3H-indole (**3**)*:*

A mixture of 4-ethenyl-3-methoxy-1-phenyl-1*H*-pyrazole (**1**) (200 mg, 1 mmol, 1 eq.) and 2-([1,1′-biphenyl]-4-yl)-5-bromo-3,3-dimethyl-3*H*-indole (**2**) (470 mg, 1.25 mmol, 1.25 eq.) was dissolved in dry dimethylformamide (2 mL) under Ar. Then, cesium carbonate (489 mg, 1.5 mmol, 1.5 eq.), tetrabutylammonium chloride (417 mg, 1.5 mmol, 1.5 eq.), and palladium(II) acetate (22 mg, 10 mol%, 0.1 mmol) were added, and the reaction mixture was stirred at 120 °C for 24 h. Upon completion, the reaction was cooled to room temperature, poured into brine (100 mL), and extracted with ethyl acetate (4 × 25 mL). Organic layers were combined, washed with brine (100 mL), dried over anhydrous sodium sulfate, and concentrated under reduced pressure. The residue was purified by column chromatography on silica gel (eluent—EtOAc/Hex 1/6 *v*/*v*) to give **3**. Yellow solid; yield 45% (223 mg); m.p. = 192–193 °C; R_f = 0.24 (EtOAc/Hex 1/6 *v*/*v*). ^{1}H NMR (700 MHz, $CDCl_3$): δ 8.25 (d, *J* = 8.5 Hz, 2H, C-Ph 3,5-H), 7.86 (s, 1H, Pyr 5-H), 7.72 (d, *J* = 8.4 Hz, 2H, C-Ph 2,6-H), 7.68–7.64 (m, 3H, Ind 7-H, Ph 2′,6′-H), 7.64–7.61 (m, 2H, N-Ph 2,6-H), 7.49–7.45 (m, 4H, Ind 4,6-H, Ph 3′,5′-H), 7.42 (dd, *J* = 8.6, 7.3 Hz, 2H, N-Ph 3,5-H), 7.38 (t, *J* = 7.4 Hz, 1H, Ph 4′-H), 7.22–7.19 (m, 1H, N-Ph 4-H), 7.18 (d, *J* = 16.3 Hz, 1H, Pyr-CH=C<u>H</u>-Ind), 6.97 (d, *J* = 16.3 Hz, 1H, Pyr-C<u>H</u>=CH-Ind), 4.13 (s, 3H, -OCH_3), 1.66 (s, 6H, Ind 3-$(CH_3)_2$). ^{13}C NMR (176 MHz, $CDCl_3$): δ 182.4 (Ind C-2), 162.5 (Pyr C-3), 152.6 (Ind C-7a), 148.3 (Ind C-3a), 143.1 (C-Ph C-1), 140.2 (Ph C-1′), 139.9 (N-Ph C-1), 136.1 (Ind C-5), 132.1 (C-Ph C-4), 129.4 (N-Ph C-3,5), 128.9 (Ph C-3′,5′), 128.8 (C-Ph C-3,5), 127.9 (Pyr-CH=<u>C</u>H-Ind), 127.8 (Ph C-4′), 127.2 (C-Ph C-2,6), 127.1 (Ph C-2′,6′), 126.1 (Ind C-6), 125.2 (N-Ph C-4), 125.0 (Pyr C-5), 120.9 (Ind C-7), 118.2 (Ind C-4), 117.5 (N-Ph C-2,6), 116.6 (Pyr-<u>C</u>H=CH-Ind), 108.5 (Pyr C-4), 56.3 (-OCH_3), 53.3 (Ind C-3), 25.0 (Ind 3-$(CH_3)_2$). ^{15}N NMR (71 MHz, $CDCl_3$): δ −70.5 (Ind N-1), −120.1 (Pyr N-2), −188.9 (Pyr N-1). IR (ATR): 3050, 3025, 3007, 2973, 2930, 2873 (CH_{arom}, CH_{aliph}), 1597, 1564, 1502, 1456, 1407, 1397, 1251, 1014, 963, 940, 847, 817, 771, 754, 736 (C=C, CH_3 bending, C-O, C-N, CH_{arom} oop bending). HRMS (*m*/*z*): $[M+H]^+$ calcd. for $C_{34}H_{30}N_3O$, 496.2383; found, 496.2392.

Supplementary Materials: 2D MDL molfile of compound **3**, Figure S1: ^{1}H NMR spectrum of compound **2**; Figure S2: ^{13}C NMR spectrum of compound **2**; Figure S3: FT-IR spectrum of compound **2**; Figure S4: HRMS spectrum of compound **2**; Figure S5: ^{1}H NMR spectrum of compound **3**; Figure S6: ^{13}C NMR spectrum of compound **3**; Figure S7: The overlaid ^{1}H–^{13}C HSQC (red) and 1,1-ADEQUATE (black) NMR spectrum of compound **3**; Figure S8: The overlaid ^{1}H–^{13}C HSQC (red) and ^{1}H–^{13}C HMBC (green) NMR spectrum of compound **3**; Figure S9: The overlaid ^{1}H–^{13}C HSQC (red) and ^{1}H–^{13}C H2BC (black) NMR spectrum of compound **3**; Figure S10: ^{1}H–^{1}H NOESY spectrum of compound **3**; Figure S11: ^{1}H–^{1}H COSY spectrum of compound **3**; Figure S12: ^{1}H–^{1}H TOCSY spectrum of compound **3**; Figure S13: ^{1}H–^{15}N LR-HSQMBC spectrum of compound **3**; Figure S14: FT-IR spectrum of compound **3**; Figure S15: HRMS spectrum of compound **3**.

Author Contributions: Conceptualization, A.B., A.Š. and G.V.; methodology, A.B., A.Š. and G.V.; formal analysis, G.V.; investigation, G.V. and A.B.; resources, A.Š.; data curation, A.B.; writing—original draft preparation, G.V.; writing—review and editing, A.Ž., N.K., A.B. and A.Š.; visualization, G.V. and A.B.; supervision, N.K.; project administration, A.Š.; funding acquisition, A.Š. All authors have read and agreed to the published version of the manuscript.

Funding: This research was funded by the Research Council of Lithuania (No. S-MIP-23-51).

Data Availability Statement: The original contributions presented in this study are included in the article/supplementary material. Further inquiries can be directed to the corresponding author(s).

Conflicts of Interest: The authors declare no conflicts of interest.

References

1. Tu, Z.; Lu, J.; Luo, X.; Hu, J.; Li, S.; Wang, Y.; Zheng, Y.; Zuo, J.; Pan, Y. Blue Axially Chiral Biphenyl Based Thermally Activated Delayed Fluorescence Materials for Efficient Circularly Polarized OLEDs. *Adv. Opt. Mater.* **2021**, *9*, 2100596. [CrossRef]
2. Zhang, Z.; Li, Y.; Wu, X.; Chu, W.; Yin, S. Solution-Processable, High Current Efficiency Deep-Blue Organic Light-Emitting Diodes Based on Novel Biphenyl-Imidazole Derivatives. *J. Mater. Chem. C* **2020**, *8*, 11239–11251. [CrossRef]
3. Xie, Y.; Han, L.; Ge, C.-S.; Cui, Y.-H.; Gao, J.-R. Novel Organic Dye Sensitizers Containing Fluorenyl and Biphenyl Moieties for Solar Cells. *Chin. Chem. Lett.* **2017**, *28*, 285–292. [CrossRef]
4. Magomedov, A.; Sakai, N.; Kamarauskas, E.; Jokubauskaitė, G.; Franckevičius, M.; Jankauskas, V.; Snaith, H.J.; Getautis, V. Amorphous Hole-Transporting Material Based on 2,2′-Bis-substituted 1,1′-Biphenyl Scaffold for Application in Perovskite Solar Cells. *Chem. Asian J.* **2017**, *12*, 958–962. [CrossRef] [PubMed]
5. Xu, Y.; Luo, Y.; Ye, J.; Liu, D.; Zhang, W. Rh-Catalyzed Enantioselective Desymmetric Hydrogenation of α-Acetamido-1,3-Indanediones Using Ether-Bridged Biphenyl Diphosphine Ligands. *J. Am. Chem. Soc.* **2023**, *145*, 21176–21182. [CrossRef] [PubMed]
6. Pedrazzani, R.; Kiriakidi, S.; Monari, M.; Lazzarini, I.; Bertuzzi, G.; López, C.S.; Bandini, M. Fluorinated Biphenyl Phosphine Ligands for Accelerated [Au(I)]-Catalysis. *ACS Catal.* **2024**, *14*, 6128–6136. [CrossRef]
7. Deng, J.; Zhang, T.; Li, B.; Xu, M.; Wang, Y. Design, Synthesis and Biological Evaluation of Biphenyl-Benzamides as Potent FtsZ Inhibitors. *Eur. J. Med. Chem.* **2022**, *239*, 114553. [CrossRef] [PubMed]
8. Singh, S.; Geetha, P.; Ramajayam, R. Isolation, Synthesis and Medicinal Chemistry of Biphenyl Analogs—A Review. *Results Chem.* **2023**, *6*, 101135. [CrossRef]
9. Wang, T.; Cai, S.; Wang, M.; Zhang, W.; Zhang, K.; Chen, D.; Li, Z.; Jiang, S. Novel Biphenyl Pyridines as Potent Small-Molecule Inhibitors Targeting the Programmed Cell Death-1/Programmed Cell Death-Ligand 1 Interaction. *J. Med. Chem.* **2021**, *64*, 7390–7403. [CrossRef] [PubMed]
10. Yao, Y.; Liao, C.; Li, Z.; Wang, Z.; Sun, Q.; Liu, C.; Yang, Y.; Tu, Z.; Jiang, S. Design, Synthesis, and Biological Evaluation of 1, 3-Disubstituted-Pyrazole Derivatives as New Class I and IIb Histone Deacetylase Inhibitors. *Eur. J. Med. Chem.* **2014**, *86*, 639–652. [CrossRef] [PubMed]
11. Asteian, A.; Blayo, A.-L.; He, Y.; Koenig, M.; Shin, Y.; Kuruvilla, D.S.; Corzo, C.A.; Cameron, M.D.; Lin, L.; Ruiz, C.; et al. Design, Synthesis, and Biological Evaluation of Indole Biphenylcarboxylic Acids as PPARγ Antagonists. *ACS Med. Chem. Lett.* **2015**, *6*, 998–1003. [CrossRef] [PubMed]
12. Sawada, J.; Osawa, A.; Takeuchi, T.; Kaneda, M.; Oishi, S.; Fujii, N.; Asai, A.; Tanino, K.; Namba, K. Functional 1,3a,6a-Triazapentalene Scaffold: Design of Fluorescent Probes for Kinesin Spindle Protein (KSP). *Bioorg. Med. Chem. Lett.* **2016**, *26*, 5765–5769. [CrossRef] [PubMed]
13. Denißen, M.; Nordmann, J.; Dziambor, J.; Mayer, B.; Frank, W.; Müller, T.J.J. Sequential Palladium Catalyzed Coupling–Cyclocondensation–Coupling (C^3) Four-Component Synthesis of Intensively Blue Luminescent Biarylsubstituted Pyrazoles. *RSC Adv.* **2015**, *5*, 33838–33854. [CrossRef]
14. Tomasulo, M.; Sortino, S.; Raymo, F.M. Bichromophoric Photochromes Based on the Opening and Closing of a Single Oxazine Ring. *J. Org. Chem.* **2008**, *73*, 118–126. [CrossRef] [PubMed]
15. Šachlevičiūtė, U.; Varvuolytė, G.; Bieliauskas, A.; Kleizienė, N.; Žukauskaitė, A.; Šačkus, A. 3,3,3′,3′-Tetramethyl-2,2′-Diphenyl-3*H*,3′*H*-5,5′-Biindole. *Molbank* **2020**, *2020*, M1146. [CrossRef]
16. Arbačiauskienė, E.; Kazlauskas, K.; Miasojedovas, A.; Juršėnas, S.; Jankauskas, V.; Holzer, W.; Getautis, V.; Šačkus, A. Pyrazolyl-Substituted Polyconjugated Molecules for Optoelectronic Applications. *Dyes Pigm.* **2010**, *85*, 79–85. [CrossRef]
17. Ali, H.A.; Ismail, M.A.; Fouda, A.E.-A.S.; Ghaith, E.A. A Fruitful Century for the Scalable Synthesis and Reactions of Biphenyl Derivatives: Applications and Biological Aspects. *RSC Adv.* **2023**, *13*, 18262–18305. [CrossRef] [PubMed]
18. Cotugno, P.; Monopoli, A.; Ciminale, F.; Cioffi, N.; Nacci, A. Pd Nanoparticle Catalysed One-Pot Sequential Heck and Suzuki Couplings of Bromo-Chloroarenes in Ionic Liquids and Water. *Org. Biomol. Chem.* **2012**, *10*, 808–813. [CrossRef] [PubMed]
19. Varvuolytė, G.; Řezníčková, E.; Bieliauskas, A.; Kleizienė, N.; Vojáčková, V.; Opichalová, A.; Žukauskaitė, A.; Kryštof, V.; Šačkus, A. Synthesis and Photodynamic Activity of New 5-[(*E*)-2-(3-Alkoxy-1-phenyl-1*H*-pyrazol-4-yl)ethenyl]-2-phenyl-3*H*-indoles. *Arch. Pharm.* **2024**, *357*, e2400282. [CrossRef] [PubMed]